Supporting Information **for**

Effects of Alkyl Chains of Benzothiadiazole-based Conjugated Polymers on the Photovoltaic Performance of Non-Fullerene Organic Solar Cells

Chao Wang,[a] Jie Fang,*[,a,b] Chong Guan,[a] Zhijie Hu,[a] Ting Wu,[a] Chengyi Xiao,*[,a] and Weiwei Li*[,a]

This document contains an update to Table S1; it replaces the previous version which was originally published on 10th January 2023

[a] Beijing Advanced Innovation Center for Soft Matter Science and Engineering & State Key Laboratory of Organic-Inorganic Composites, Beijing University of Chemical Technology, Beijing 100029, P.R. China. E-mail: fangj17@lzu.edu.cn, xiaocy@mail.buct.edu.cn and liweiwei@iccas.ac.cn

[b] Institute of Applied Chemistry, Jiangxi Academy of Sciences, Nanchang 330096.

Contents

1. Materials and measurements

The synthetic procedures were performed under an argon atmosphere. Commercial chemicals (from *Sigma-Aldrich*, *J&K Chemical*, and *TCI*) were used as received. ^{1}H-NMR and ^{13}C-NMR spectra of intermedia products and monomers were recorded at 400 MHz and 600 MHz on a *Bruker* AVANCE spectrometer with TMS as the internal standard. Cyclic voltammetry was performed under an inert atmosphere at a scan rate of 0.1 V/s and 1 M tetrabutylammonium hexafluorophosphate in acetonitrile as the electrolyte, a glassy-carbon working electrode coated with samples, a platinum-wire auxiliary electrode, and an Ag/AgCl as a reference electrode. Thermogravimetric analysis data were obtained from a TGA8000 Thermogravimetric Analyzer (PerkinElmer).

Solar cells. OSCs use conventional device configuration as ITO/PEDOT:PSS/active layer/PFN-Br/Ag. Photovoltaic devices were made by spin-coating the PEDOT:PSS aqueous solution through a 0.45 mm filter, at 6000 rpm for 40 s onto pre-cleaned, patterned ITO substrates and then heating the ITO substrate in the air at 150 °C annealing for 0.5 h. The polymer donor:L8-BO (D:A = 1:1.2, 16 mg/mL in total) was dissolved in chloroform (CF) with 1, 3-dibromo-5-chlorobenzene (DBCl) (12 mg/mL) additive. The blended solution was spin-coated on the PEDOT:PSS layer at 3000 rpm for 40 seconds. It was then annealed at 100 °C for 10 minutes. Then PFN-Br methanol solution with a concentration of 1.0 mg/mL was deposited on the active layer at a speed of 3500 rpm for 30 s to provide a PFN-Br cathode modification layer. The thin films were then transferred into the N_2-filled glove box. 80 nm of Ag layer were then deposited onto the active layer by shadow masks. The thickness of the active layer is about 100 nm.

The active area of the cells was 0.04 cm^2. The *J-V* characteristics were measured by a Keithley 2400 source meter unit under an AM1.5G spectrum from a solar simulator (Enlitech model SS-F5-3A). Solar simulator illumination intensity was determined at 100 mW/cm^2 using a monocrystal silicon reference cell with a KG5 filter. Short circuit currents under AM1.5G conditions were estimated from the spectral response and convolution with the solar spectrum. The external quantum efficiency was measured by a Solar Cell Spectral Response Measurement System QE-R3011 (*Enli Technology* Co., Ltd.). The thickness of the active layers in the photovoltaic devices was measured on a Veeco Dektak XT profilometer.

SCLC. Space-charge-limited-current (SCLC) measurements were carried out using a Keithley 2400 source/measure. Electron-only devices were constructed using the ITO/PEDOT:PSS/active layer/MoO_3/Ag architecture, while hole-only devices were constructed using the ITO/ZnO/active layer/PFN-Br/Ag architecture. Current-voltage sweeps were carried out in the region of -6 V to 6 V in steps of 0.03 V at a slow rate. The carrier mobilities were measured using the space-charge-limited-current (SCLC) model, which is described by:

$$J = \frac{9}{8}\varepsilon_0\varepsilon_r\mu\frac{V^2}{L^3} \qquad \textbf{(eq. 1)}$$

Where J is the current density, ε_0 is the permittivity of the vacuum (8.85×10^{-12} F/m), ε_r is the dielectric constant of the polymer, and L is the thickness of the polymer layer, μ is the hole or electron mobility, V is the internal voltage in the device and $V = V_{appl} - V_r - V_{bi}$, where V_{appl} is the applied voltage to the device, V_r is the voltage drop due to contact resistance and series resistance across the electrodes, and V_{bi} is the built-in voltage due to the relative work function difference of the two electrodes. The thickness of the BHJ blend for SCLC measurement was about 100 nm. The hole/electron mobilities were calculated with the *Mott-Gurney* equation in the SCLC region (slope = 2 in log$J$ vs log$V$ plots). [S1, 2]

GIWAX. GIWAXS measurements were conducted on a Xenocs-SAXS/WAXS system with an X-ray wavelength of 1.5418 Å. The film samples were irradiated at a fixed angle of 0.2°. All film samples were prepared by spin-coating CF/1-CN solutions on Si substrates.

AFM. Atomic force microscopy (AFM) images were recorded using a Digital Instruments Nanoscope IIIa multimode atomic force microscope in tapping mode under ambient conditions.

2. Synthesis

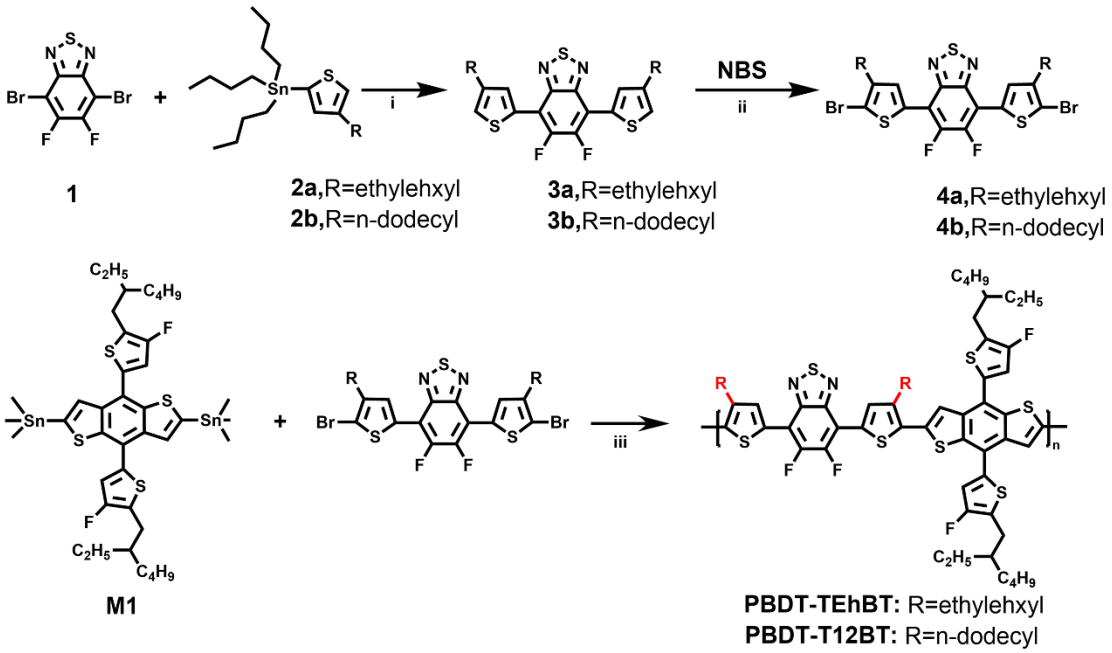

Scheme S1. Synthetic routes for BT-based donors. (i) $Pd(PPh_3)_4$, Toluene, 115 °C. (ii) NBS, THF, room temperature. (iii) $Pd(PPh_3)_4$, Toluene, 115 °C.

Synthesis of Compound 3a. A mixture of compound **1** (500 mg, 1.51 mmol) and compound **2a** (1.89 g, 4.26 mmol) in 15 mL of toluene was degassed three times, followed by the addition of $Pd(PPh_3)_4$ (46.21 mg, 0.04 mmol) as a catalyst. The reaction mixture was stirred under the protection of N_2 for 14 h at 110 °C. Then, the mixture was cooled and extracted with dichloromethane. The organic layer was combined and dried with anhydrous Na_2SO_4. After the removal of the solvent, the crude product was purified by a silica gel using petroleum ether as eluents to give compound **3a** (421.89 mg，49.82%). ^{1}H NMR ($CDCl_3$, 400 MHz): δ (ppm) 8.09 (s, 2H), 7.186 (s, 2H), 2.667-2.655 (d, J = 4.8 Hz, 4H), 1.664-1.644 (t, J = 8.96 Hz, 2H), 1.541-1.257 (m, J = 113.6 Hz, 17H), 0.933-0.891 (t, J = 14.8 Hz, 8H), 0.883-0.918 (t, J = 16.8 Hz, 12H).

Synthesis of Compound 3b. A mixture of compound **1** (615 mg, 1.86 mmol) and compound **2b** (1.89 g, 4.60 mmol) in 15 mL of toluene was degassed three times, followed by the addition of $Pd(PPh_3)_4$ (57.76 mg, 0.05 mmol) as a catalyst. The reaction mixture was stirred under the protection of N_2 for 14 h at 110 °C. Then, the mixture was cooled and extracted with dichloromethane. The organic layer was combined and dried with anhydrous Na_2SO_4. After the removal of the solvent, the crude product was

purified by a silica gel using petroleum ether as eluents to give compound **3b** (510 mg，40.78%). ^{1}H NMR ($CDCl_3$, 400 MHz): δ (ppm) 8.124 (s, 2H), 7.209 (s, 2H), 2.737-2.699 (t, J = 15.2 Hz, 4H), 1.722-1.667 (t, J = 22 Hz, 4H), 1.389-1.261 (m, J = 51.2 Hz, 42H), 0.893-0.859 (t, J = 13.6 Hz, 6H).

Synthesis of Compound 4a. Compound **3a** (348.3 mg, 0.62 mmol) and *N*-bromosuccinimide (NBS) (334.37 mg, 1.86 mmol) were placed in a 50 ml round-bottom flask, dissolved by adding 20 mL of THF, and stirred for 24 hours at room temperature under dark conditions. After the completion of the reaction, the reaction system was poured into a 100 mL saturated $NaHCO_3$ aqueous solution, extracted with methylene chloride, and the recovered organic layer was dried with anhydrous Na_2SO_4. After the removal of the solvent, the crude product was purified by a silica gel using petroleum ether as eluents to give compound **4a** (420 mg，94.18%). ^{1}H NMR ($CDCl_3$, 400 MHz): δ (ppm) 7.932 (s, 2H), 2.611-2.593 (d, J = 7.2 Hz, 4H), 1.721-1.691 (t, J = 12 Hz, 2H), 1.406-1.320 (m, J = 34.4 Hz, 18H), 0.947-0.881 (t, J = 26.4 Hz, 12H). ^{13}C NMR (600 MHz, $CDCl_3$) δ (ppm) 150.612, 150.474, 148.885, 148.747, 148.458, 148.431, 141.792, 132.354, 132.323, 131.061, 115.098, 111.075, 111.012, 40.000, 33.761, 33.761, 32.485, 28.780, 25.720, 23.082, 14.153, 10.872. (HR-MALDI-TOF): *m*/*z*: 717.89. (calcd for $C_{30}H_{36}Br_2F_2N_2S_2$: 718.04)

Synthesis of Compound 4b. Compound **3b** (268 mg, 0.40 mmol) and *N*-bromosuccinimide (214.4 mg, 1.19 mmol) were placed in a 50 mL round-bottom flask, dissolved by adding 20 mL of THF, and stirred for 24 hours at room temperature under dark conditions. After the completion of the reaction, the reaction system was poured into a 100 mL saturated $NaHCO_3$ aqueous solution, extracted with methylene chloride, and the recovered organic layer was dried with anhydrous Na_2SO_4. After removal of the solvent, the crude product was purified by a silica gel using petroleum ether as eluents to give compound **4b** (145 mg，43.67%). ^{1}H NMR ($CDCl_3$, 400 MHz): δ (ppm) 7.967 (s, 2H), 2.682-2.644 (t, J = 15.2 Hz, 4H), 1.687-1.651 (t, J = 14.4 Hz, 4H), 1.361-1.258 (t, J = 41.2 Hz, 40H), 0.891-0.857 (t, J = 13.6 Hz, 6H). ^{13}C NMR (600 MHz, $CDCl_3$) δ (ppm) 150.612, 148.887, 148.442, 142.645, 131.828, 131.795, 131.239, 114.456, 111.036, 31.936, 29.763, 29.697, 29.661, 29.601, 29.560, 29.435, 29.371,

29.255, 22.703, 14.130. (HR-MALDI-TOF): *m*/*z*: 823.26. (calcd for $C_{102}H_{118}N_{10}O_2S_4$: 828.16).

Synthesis of polymer PBDT-TEhBT. Monomer **4a** (74.56 mg, 0.1 mmol), **M1** (97.67 mg, 0.1 mmol), and $Pd(PPh_3)_4$ (5.78 mg, 5 μmol) were combined in a 100 mL sealed tube. Dry toluene (3 mL) was added under the N_2 atmosphere. The mixture was stirred at 115 °C for 48 h. After cooling down to room temperature, the reactant mixture was poured into methanol (30 mL) and filtered through a Soxhlet cannula, and washed with acetone, hexane, and dichloromethane. The polymer was dissolved by 50 mL chlorobenzene. The chlorobenzene solution was then concentrated by evaporation and precipitated into acetone. The solid was collected by filtration and dried in vacuo to obtain the polymer into a dark solid (62.38 mg, 36.03%).

Synthesis of polymer PBDT-T12BT. Monomer **4b** (54.43 mg, 0.07 mmol), **M1** (61.51 mg, 0.07 mmol), and $Pd(PPh_3)_4$ (4.04 mg, 3.5 μmol) were combined in a 100 mL sealed tube. Dry toluene (3 mL) was added under the N_2 atmosphere. The mixture was stirred at 115 °C for 48 h. After cooling down to room temperature, the reactant mixture was poured into methanol (30 mL) and filtered through a Soxhlet cannula, and washed with acetone, hexane, and dichloromethane. The polymer was dissolved by 50 mL chlorobenzene. The chlorobenzene solution was then concentrated by evaporation and precipitated into acetone. The solid was collected by filtration and dried in vacuo to get the polymer into a dark solid (50.76 mg, 43.78%).

3. Statistical Reference

Table S1. The statistical reference of NFA-OSCs based on BT-series polymer donors.

Materials	V_{OC} (V)	E_g[a] (eV)	V_{loss}[b] (V)	PCE (%)	Reference
PffBT4T-2OD:BAF-4CN	0.77	1.64	0.87	8.40	S3
PffBT4T-2OD:BAF-2HDT	0.77	1.65	0.88	7.13	S4
PffBT4T-2OD:BTTIC	0.86	1.51	0.65	10.18	S5
PffBT4T-2OD:FBR	1.11	1.61	0.50	6.74	S6
PffBT4T-2OD:EH-IDTBR	1.04	1.62	0.58	9.40	S7
PffBT4T-2OD:rr-PBN	0.93	1.61	0.68	5.25	S8
PffBT4T-2OD:ITIC-Th	0.85	1.59	0.74	6.20	S9
PffBT4T-2OD:bis-PDI	0.85	1.63	0.78	5.02	S10
PffBT4T-2OD:SF(BR)4	0.93	1.61	0.68	4.61	S11
PffBT4T-2DT:IDTBR	1.07	1.60[c]	0.53	9.95	S12
PffBT4T-2DT:FBR	1.12	1.62[a]	~0.50[d]	7.80	S12
PffBT4T-2OD:EH-IDTBR	1.08	1.62	0.54	9.50	S13
PffBT4T-2DT:EH-IDTBR	1.02	1.64	0.62	11.10	S14
PffBT4T-2OD:ZITI-N-EH	0.805	1.40[c]	0.59[d]	13.07	S15
PffBT2TTT:O-IDTBR	1.08	1.63[c]	0.55[d]	10.10	S16
PffBT2TTVT:ITIC	0.78	1.58[c]	0.80[d]	3.69	S17
PffBT2TETVT:ITIC	0.91	1.58[c]	0.67[d]	8.18	S17
PffBT2TETVT(5):ITIC	0.99	1.59	0.60	6.80	S18
PffBT2TETVT(5):IDIC	0.90	1.59	0.69	8.50	S18
PffBT2TETVT(6):ITIC	0.90	1.59	0.69	6.90	S18
PffBT2TETVT(6):IDIC	0.78	1.59	0.81	6.80	S18
P3TEA(OD):SF-PDI2	1.11	1.63	0.52	9.50	S19
2TRA:IEICO-4F	0.73	1.28	0.55	12.10	S20
PPDT2FBT:BTDT2R	1.07	1.74	0.67	6.90	S21

PBDT-ffBT-T:ITIC-Th	0.92	1.60	0.68	8.59	S22
PDTP-DFBT:FOIC	0.71	1.31	0.60	4.20	S23
PfBTAZ:O-IDTBR	1.00	1.58	0.58	7.50	S24
PfBTAZS:O-IDTBR	0.98	1.57	0.59	10.10	S24
PBT-BTrTa(T):ICz-Rd2	1.04	1.34	0.30	7.88	S25
PBT-BTrTa(T):ICz-RdCN2	1.01	1.33	0.32	9.76	S25
P104:ITIC-4F	0.83	1.34	0.51	8.32	S26
P105:ITIC-4F	0.91	1.34	0.43	10.65	S26
PPhI-ffBT:ITIC-4F	0.91	1.52[c]	0.61[d]	13.31	S27
PffPhI-ffBT:ITIC-4F	0.94	1.52[c]	0.58[d]	12.74	S27
PBDT-TEhBT:L8-BO	**0.90**	**1.38**	**0.48**	**15.55**	**This work**

[a] $E_g = 1240/\lambda_{onset}$, here λ_{onset} is the onset of the EQE spectra. [b]Calculated from the E_g/q - V_{OC}. [c] E_g calculated from the optical absorptions. [d]Data acquired directly from the literature.

4. GPC, Absorption, DSC and CV

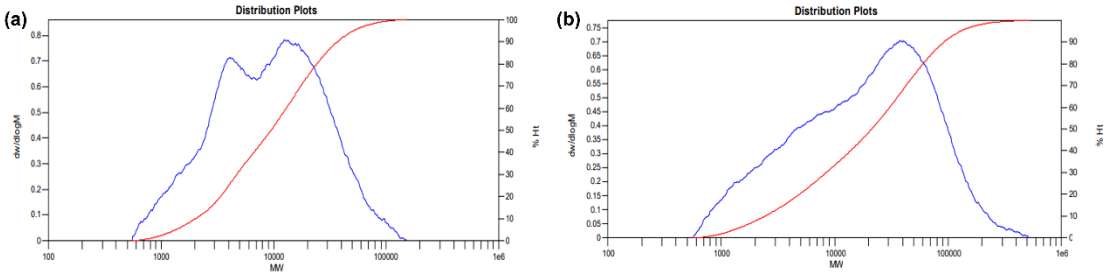

Figure S1. (a) GPC curve of PBDT-T12BT recorded at 150 °C with *o*-DCB as eluent. (b) GPC curve of PBDT-TEhBT recorded at 150 °C with *o*-DCB as eluent.

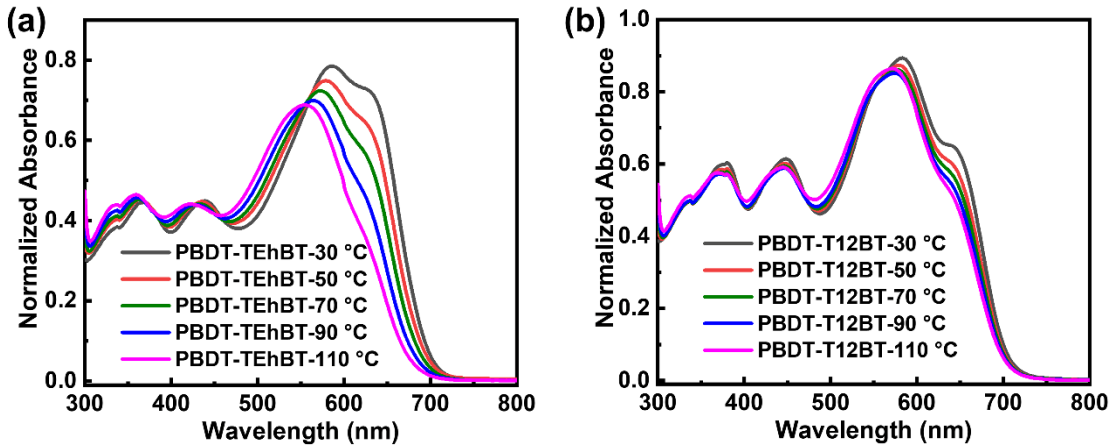

Figure S2. Normalized temperature-dependent absorption spectra of (a) PBDT-TEhBT and (b) PBDT-T12BT in chloroform solutions.

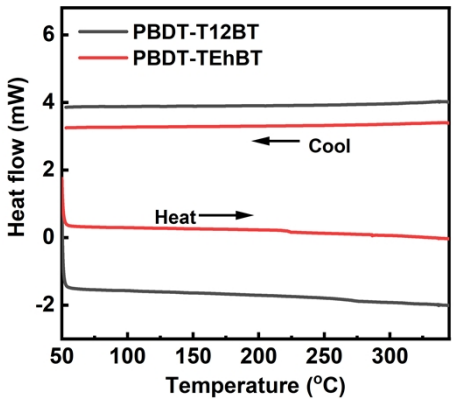

Figure S3. DSC heating and cooling traces (second cycle) at a scanning rate of 10 °C/min under an N_2 atmosphere.

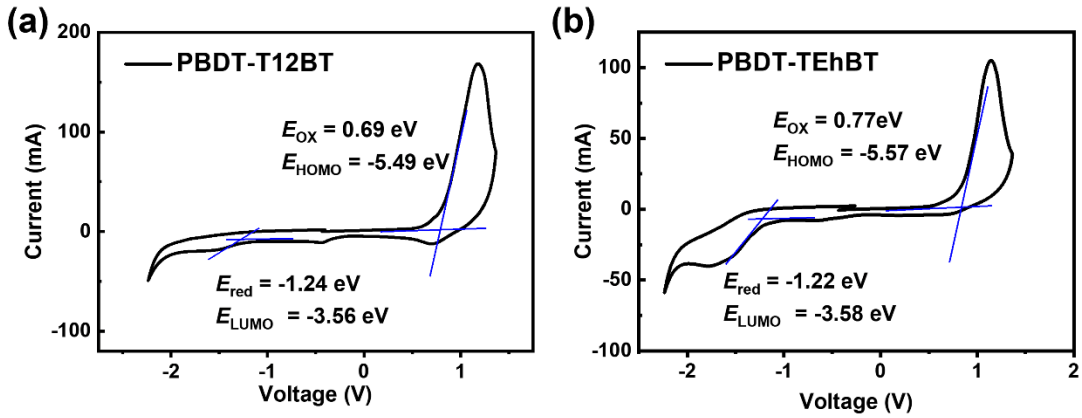

Figure S4. Cyclic voltammogram measured in thin films of (a) PBDT-T12BT, (b) PBDT-TEhBT thin film. Potential vs. Fc/Fc^{+}. $E_{HOMO} = -(E_{onset} + 4.8)$ eV; $E_{LUMO} = -(E_{onset} + 4.8)$ eV.

5. Organic Solar Cells

Table S2. The solar cell optimization is based on the photoactive layers spin-coated from different solvents. The thickness of the active layers is ~100 nm.

	Solvent	J_{SC} (mA/cm^2)	V_{OC} (V)	FF	PCE (%)
PBDT-T12BT:L8-BO	CB	16.18	0.77	0.34	4.24
	CF	17.78	0.77	0.38	5.16
	CF/0.5%CN	15.97	0.77	0.42	5.08
	CF/1%CN	15.13	0.77	0.42	5.12
	CF/12%DBCl	16.87	0.79	0.43	5.75
	CF/18%DBCl	15.30	0.78	0.42	5.02
PBDT-TEhBT:L8-BO	CB	26.39	0.88	0.46	10.66
	CF	24.36	0.89	0.57	12.18
	CF/0.5%CN	25.81	0.89	0.58	13.15
	CF/1%CN	24.36	0.88	0.60	12.85
	CF/12%DBCl	24.53	0.90	0.70	15.55
	CF/18%DBCl	23.41	0.91	0.69	14.75

Table S3. The solar cell optimization is based on the photoactive layers with different annealing temperatures and thicknesses.

	TA Annealing (°C)	Thickness (nm)	J_{SC} (mA/cm^2)	V_{OC} (V)	FF	PCE (%)
PBDT-T12BT:L8-BO	25	123	13.89	0.80	0.43	4.74
	100	106	16.87	0.79	0.43	5.75
	150	85	16.43	0.79	0.41	5.32
PBDT-TEhBT:L8-BO	25	124	25.94	0.89	0.63	14.46
	100	110	24.53	0.90	0.70	15.55
	150	96	24.53	0.90	0.67	14.87

Table S4. Photovoltaic parameters of 6 devices based on PBDT-T12BT:L8-BO fabricated from CF/12% DBCl at 100 °C.

No.	J_{SC} (mA/cm^2)	V_{OC} (V)	FF	PCE (%)
1	16.92	0.79	0.42	5.59
2	17.78	0.77	0.38	5.16
3	16.59	0.78	0.42	5.40
4	15.13	0.77	0.43	5.01
5	16.24	0.79	0.42	5.39
6	16.87	0.79	0.43	5.75
average	16.59±0.88	0.78±0.01	0.42±0.02	5.38±0.27

Table S5. Photovoltaic parameters of 6 devices based on PBDT-TEhBT:L8-BO fabricated from CF/12% DBCl at 100 °C.

No.	J_{SC} (mA/cm^2)	V_{OC} (V)	FF	PCE (%)
1	26.12	0.90	0.66	15.38
2	24.73	0.90	0.64	14.34
3	24.20	0.90	0.67	14.45
4	22.99	0.90	0.69	14.38
5	24.00	0.91	0.69	15.00
6	24.53	0.90	0.70	15.55
average	24.43±1.02	0.90±0.004	0.68±0.02	14.85±0.54

Table S6. Photovoltaic parameters of OSCs based on different donor polymers and acceptors fabricated from CF/12% DBCl at 100 °C.

	V_{OC} (V)	J_{SC} (mA/cm^2)	FF	PCE (%)
PBDT-T12BT:Y6	0.77	15.90	0.53	6.47
PBDT-T12BT:BTP-BO-4Cl	0.76	15.36	0.53	6.21
PBDT-TEhBT:Y6	0.86	23.88	0.74	15.23
PBDT-TEhBT:BTP-BO-4Cl	0.86	24.68	0.71	15.18

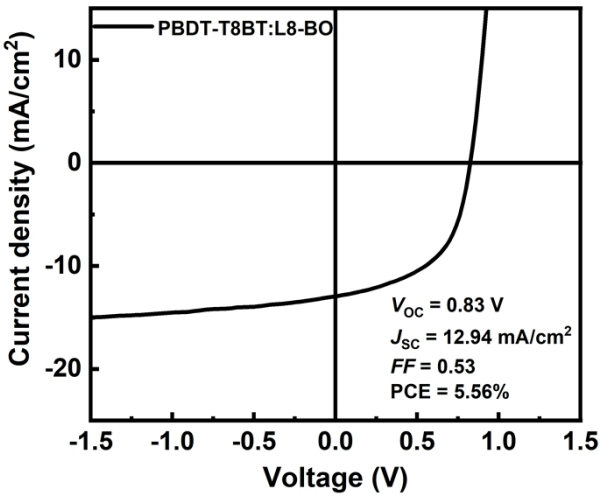

Figure S5. *J-V* characteristics of OSCs based on PBDB-T8BT:L8-BO under AM1.5G illumination.

6. AFM phase

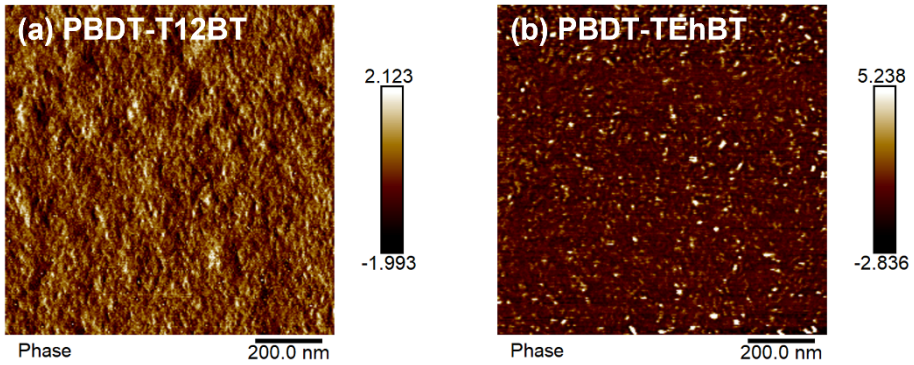

Figure S6. AFM phase images of (a) PBDT-T12BT, (b) PBDT-TEhBT thin films.

7. NMR and HR-MALDI of the compounds

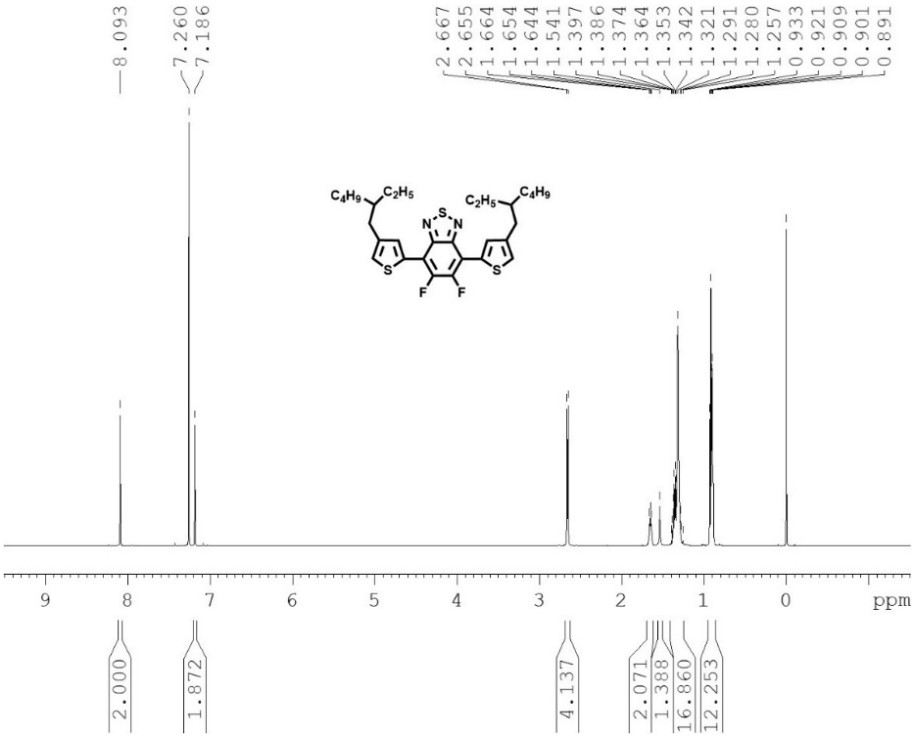

Figure S7. ^{1}H-NMR of compound **3a** recorded in $CDCl_3$.

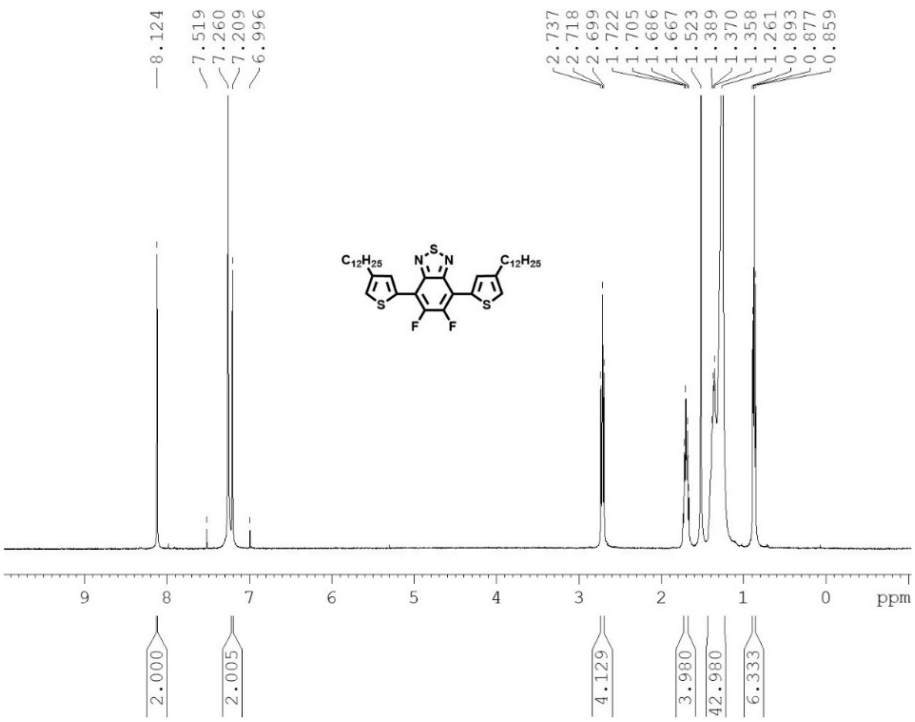

Figure S8. ^{1}H-NMR of compound **3b** recorded in $CDCl_3$.

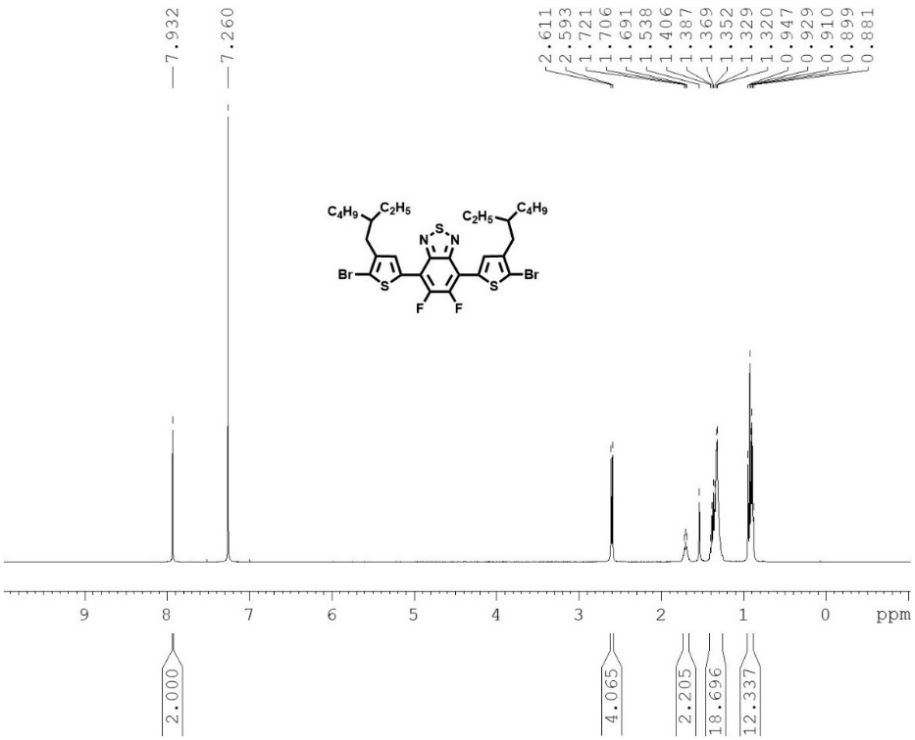

Figure S9. ^{1}H-NMR of compound **4a** recorded in $CDCl_3$.

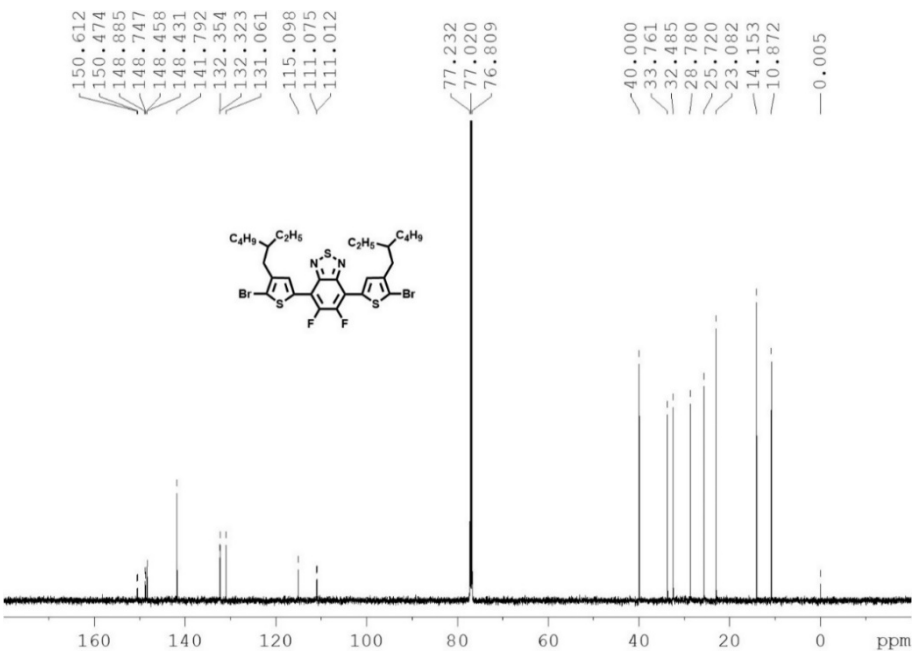

Figure S10. ^{13}C-NMR of compound **4a** recorded in $CDCl_3$.

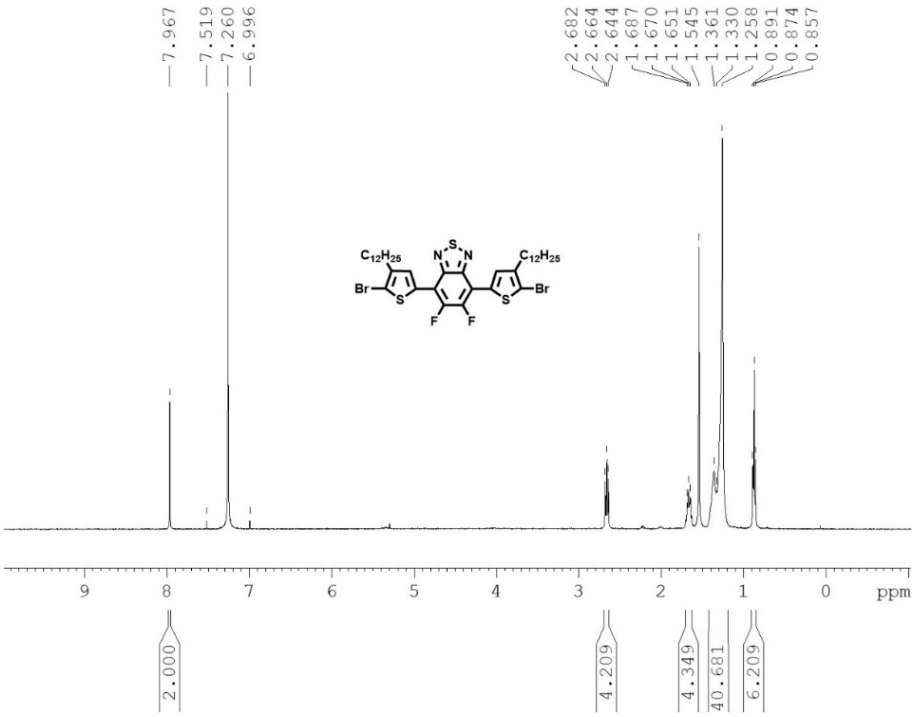

Figure S11. ^{1}H-NMR of compound **4b** recorded in $CDCl_3$.

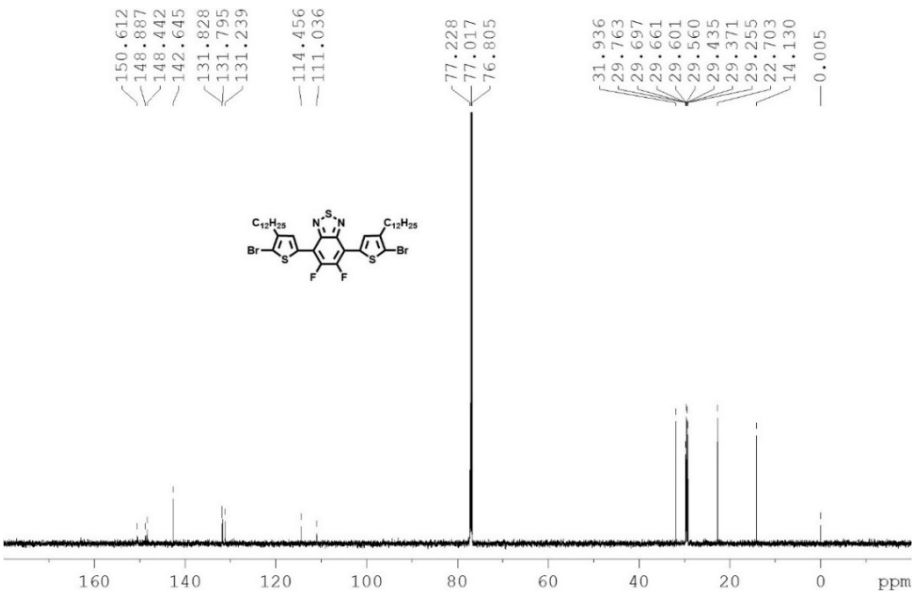

Figure S12. ^{13}C-NMR of compound **4b** recorded in $CDCl_3$

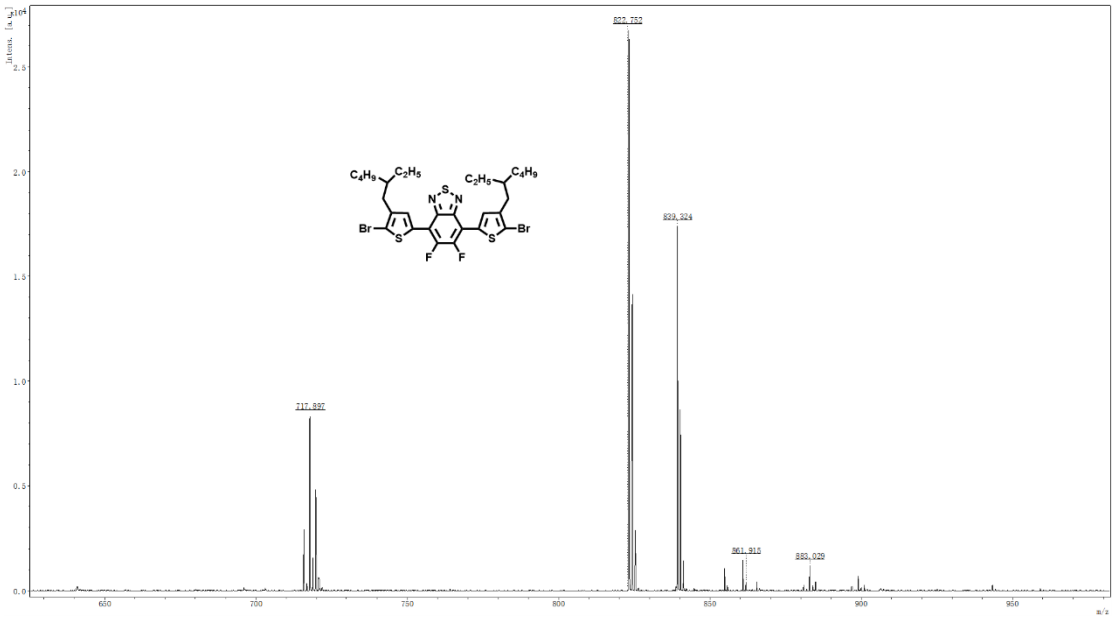

Figure S13. HR-MALDI of compound **4a** recorded in $CDCl_3$.

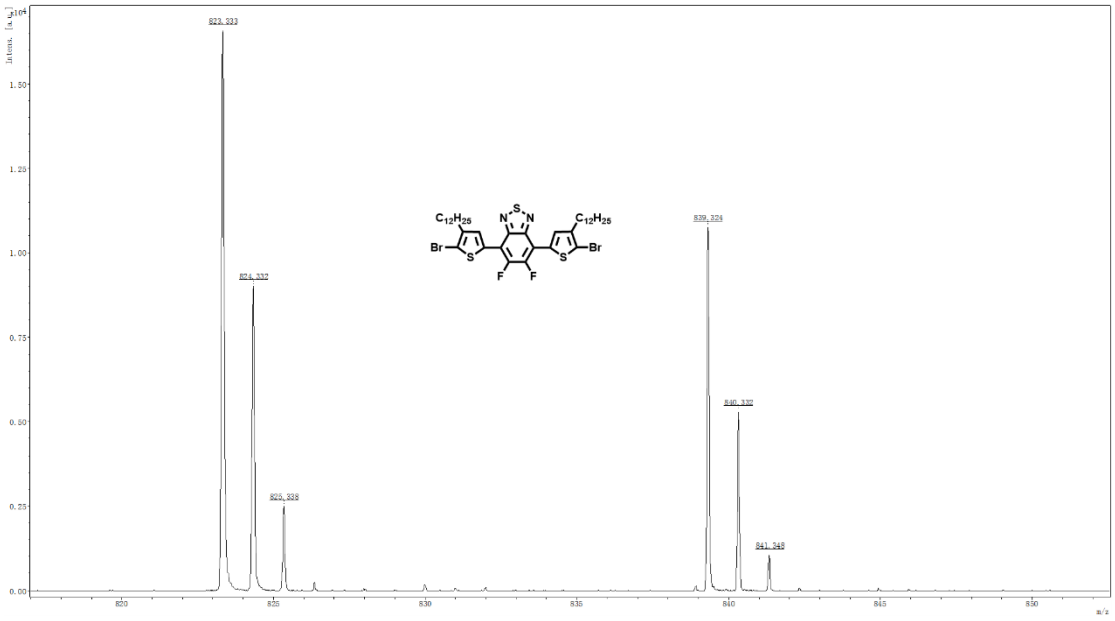

Figure S14. HR-MALDI of compound **4b** recorded in $CDCl_3$.

8. Reference

S1. N. F. Mott and R. W. Gurney, *Electronic processes in ionic crystals*, Clarendon Press, 1948.

S2. P. N. Murgatroyd, *J. Phys. D: Appl. Phys.*, 1970, **3**, 151-156.

S3. Suman, V. Gupta, A. Bagui and S. P. Singh, *Adv. Funct. Mater.*, 2017, **27**, 1603820.

S4. Suman, A. Bagui, V. Gupta, K. K. Maurya and S. P. Singh, *J Phys Chem C*, 2016, **120**, 24615-24622.

S5. T. Liu, W. Gao, G. Zhang, L. Zhang, J. Xin, W. Ma, C. Yang, H. Yan, C. Zhan and J. Yao, *Sol. RRL*, 2019, **3**, 1800376.

S6. H. Cha, S. Wheeler, S. Holliday, S. D. Dimitrov, A. Wadsworth, H. H. Lee, D. Baran, I. McCulloch and J. R. Durrant, *Adv. Funct. Mater.*, 2018, **28**, 1704389.

S7. G. C. Zhang, R. X. Xia, Z. Chen, J. Y. Xiao, X. N. Zhao, S. Y. Liu, H. L. Yip and Y. Cao, *Adv. Energy Mater.*, 2018, **8**, 1801609.

S8. R. Zhao, B. Lin, J. Feng, C. Dou, Z. Ding, W. Ma, J. Liu and L. Wang, *Macromolecules*, 2019, **52**, 7081-7088.

S9. H. Hu, K. Jiang, P. C. Y. Chow, L. Ye, G. Zhang, Z. Li, J. H. Carpenter, H. Ade and H. Yan, *Adv. Energy Mater.*, 2018, **8**, 1701674.

S10. R. Singh, S. R. Suranagi, J. Lee, H. Lee, M. Kim and K. Cho, *Sci. Rep.*, 2018, **8**, 2849.

S11. H. Tan, Y. Long, J. Zhang, J. Zhu, J. Yang, J. Yu and W. Zhu, *Dyes Pigm.*, 2019, **162**, 797-801.

S12. D. Baran, T. Kirchartz, S. Wheeler, S. Dimitrov, M. Abdelsamie, J. Gorman, R. S. Ashraf, S. Holliday, A. Wadsworth, N. Gasparini, P. Kaienburg, H. Yan, A. Amassian, C. J. Brabec, J. R. Durrant and I. McCulloch, *Energy Environ. Sci.*, 2016, **9**, 3783-3793.

S13. H. Cha, J. Wu, A. Wadsworth, J. Nagitta, S. Limbu, S. Pont, Z. Li, J. Searle, M. F. Wyatt, D. Baran, J.-S. Kim, I. McCulloch and J. R. Durrant, *Adv. Mater.*, 2017, **29**, 1701156.

S14. A. Wadsworth, R. S. Ashraf, M. Abdelsamie, S. Pont, M. Little, M. Moser, Z. Hamid, M. Neophytou, W. Zhang, A. Amassian, J. R. Durrant, D. Baran and I. McCulloch, *ACS Energy Lett.*, 2017, **2**, 1494-1500.

S15. J. Y. Zhang, W. R. Liu, M. Zhang, S. J. Xu, F. Liu and X. Z. Zhu, *J. Mater. Chem. A*, 2020, **8**, 8661-8668.

S16. S. Chen, Y. Wang, L. Zhang, J. Zhao, Y. Chen, D. Zhu, H. Yao, G. Zhang, W. Ma, R. H. Friend, P. C. Y. Chow, F. Gao and H. Yan, *Adv. Mater.*, 2018, **30**, e1804215.

S17. X. Wang, A. Tang, F. Chen and E. Zhou, *Macromolecules*, 2018, **51**, 4598-4607.

S18. S. J. Jeon, Y. W. Han and D. K. Moon, *ACS Appl. Mater. Interfaces*, 2019, **11**, 9239-9250.

S19. G. Yang, J. Liu, L.-K. Ma, S. Chen, J. Y. L. Lai, W. Ma and H. Yan, *Mater. Chem. Front.*, 2018, **2**, 1360-1365.

S20. Z. Chen, Z. Hu, Y. Liang, C. Zhou, J. Xiao, G. Zhang and F. Huang, *Org. Electron.*, 2020, **85**, 105874.

S21. J. Ahn, S. Oh, H. Lee, S. Lee, C. E. Song, H. K. Lee, S. K. Lee, W.-W. So, S.-J. Moon, E. Lim, W. S. Shin and J.-C. Lee, *ACS Appl. Mater. Interfaces*, 2019, **11**, 30098-30107.

S22. Y. Xin, G. Zeng, J. Zhang, X. Zhao and X. Yang, *J. Mater. Chem. A*, 2018, **6**, 9561-9568.

S23. Y. Xie, R. Xia, T. Li, L. Ye, X. Zhan, H.-L. Yip and Y. Sun, *Small Methods*, 2019, **3**, 1900424.
S24. S. Chen, L. Zhang, C. Ma, D. Meng, J. Zhang, G. Zhang, Z. Li, P. C. Y. Chow, W. Ma, Z. Wang, K. S. Wong, H. Ade and H. Yan, *Adv. Energy Mater.*, 2018, **8**, 1702427.
S25. Suman, A. Siddiqui, M. L. Keshtov, G. D. Sharma and S. P. Singh, *J. Mater. Chem. C*, 2019, **7**, 543-552.
S26. M. L. Keshtov, S. A. Kuklin, A. R. Khokhlov, Z. Xie, C. Dou, Y. Zou, I. E. Ostapov, E. E. Makhaeva, R. Suthar and G. D. Sharma, *ACS Appl. Energy Mater.*, 2020, **3**, 495-505.
S27. J. Yu, P. Chen, C. W. Koh, H. Wang, K. Yang, X. Zhou, B. Liu, Q. Liao, J. Chen, H. Sun, H. Y. Woo, S. Zhang and X. Guo, *Adv. Sci.*, 2019, **6**, 1801743.